Iranian Journal of Materials Forming 9 (4) (2022) 26-33

Online ISSN: 2383-0042

IJMF

Iranian Journal of Materials Forming

Journal Homepage: http://ijmf.shirazu.ac.ir

Research Article

Finite Element Analysis of Phase Distribution in Forging of the Two-Phase Ti-6Al-4V Alloy to have a Hip Joint Implant

H. Gheshlaghi[1], V. Alimirzaloo[1], M. Shahbaz[2*] and A. Amiri[3]

[1] Department of Mechanical Engineering, Faculty of Engineering, Urmia University, Urmia 15311-57561, Iran
[2] Department of Materials Science and Engineering, Faculty of Engineering, Urmia University, Urmia 15311-57561, Iran
[3] Mechanical Engineering Department, Islamic Azad University, North Tehran Branch, Tehran, Iran

ARTICLE INFO

Article history:

Received 21 August 2022
Reviewed 19 Septemer 2022
Revised 22 September 2022
Accepted 27 September 2022

Keywords:

Hip joint implant
Ti-6Al-4V
Finite element analysis
Phase distribution

Please cite this article as:

H. Gheshlaghi, V. Alimirzaloo, M. Shahbaz, A. Amiri, Finite element analysis of phase distribution in forging of the two-phase Ti-6Al-4V alloy to have a hip joint implant, *Iranian Journal of Materials Forming*, 9(4) (2022) 26-33.

ABSTRACT

In this research, the finite element analysis (FEA) of the effect of forging parameters including temperature, strain rate and cooling rate on the percentage of α and β phases in forging of the two-phase Ti-6Al-4V alloy to fabricate a hip joint implant was investigated. In order to be used in FEA, the stress-strain curves of Ti-6Al-4V at temperatures ranged between 800 to 1000℃ and, strain rates of 0.01, 0.1, 1 s^{-1} up to a total strain of 0.45 by using hot compression test were obtained. The force-displacement curve of hot compression test of a cylindrical sample made of Ti-6Al-4V alloy from FEA and experiment in similar condition was used for verification. Results showed that all three input variables have an effect on the volume percentage of final α and β phases. By increasing the cooling rate, forging temperature and strain rate, the percentage of the final α phase decreases and the amount of the β phase increases. Additionally, in all cooling rates, the amount of the final α phase decreases from the center to the sides of samples.

1. Introduction

Titanium alloy Ti-6Al-4V is widely used in medical applications because of its excellent strength, osseointergration, biocompatibility [1], high strength to weight ratio, and good corrosion resistance [2]. Microstructural evolutions such as phase transformation and distribution, average grain size, grain distribution and texture directly influence the mechanical properties of processed materials. Determining and controlling the microstructural evolution is, hence, important in order to obtain desired properties at each thermomechanical step and in the final products. In the meantime, phase percentage plays a crucial role in the successive performance of the materials under mechanical loadings. As it is known, Ti-6Al-4V is a two-phase alloy

* Corresponding author
E-mail address: m.shahbaz@urmia.ac.ir (M. Shahbaz)
https://doi.org/10.22099/IJMF.2022.44610.1238

consisting of α and β phases at room temperature, which can achieve varieties of properties by changing their characteristics. Mechanical properties of this material strongly depend on the initial condition of the as-received material and processing parameters.

There is some research which mostly investigates the effects of phase distribution in Ti-6Al-4V alloys on fatigue behavior of the alloy. Nalla et al. [3] investigated the influence of two various microstructures, bimodal versus lamellar on high-cycle fatigue (HCF) of Ti-6Al-4V. Zuo et al. [4] analyzed the fatigue behavior of two different microstructures, the bimodal and basketweave for Ti-6Al-4V alloy. Wu et al. [5] analyzed the effect of microstructural condition on the high cycle fatigue (HCF) properties of the Ti-6Al-4V alloy. Crupi et al. [6] studied the effects of microstructure (α + β and β) on very high cycle fatigue behavior of the Ti-6Al-4V alloy. However, due to the excellent properties of Ti-6Al-4V, its compatibility with body tissue [7], lack of toxic ions, elasticity modulus near the bone elasticity and the perfect fatigue life [8], it is considered as the first choice in medical industries such as manufacturing of artificial hip joints, dental implants and other surgical implants [9-11]. Meanwhile, due to the vast demand for artificial implants in the medical industry, hip joints from Ti-6Al-4V are promptly increasing and many investigations have been carried out in this regard [12-15]. Some methods such as forging, casting and machining have been applied to construct the artificial hip joints. However, due to the higher strength, ability of production of geometrically complicated parts, resistance to impact, lack of defects, strength in a desired direction and low porosity, the hot forging process with perceive die can be considered as an effective method to manufacture artificial hip joints [16, 17].

To evaluate the influence of the hot forging process variables such as flash geometry, temperature, frictional condition and cooling rate on the phases volume and distribution, it is valuable to perform this process numerically before the actual manufacturing takes place. This paper presents a thermomechanical simulation of the forging of artificial hip joints for two phases of the Ti-6Al-4V alloy. Due to the importance of the α phase on the hot forged hip joints from Ti-6Al-4V, α percentage and its distribution need to be investigated. Moreover, it was found that, the former studies have not focused on α phase distribution of the Ti-6Al-4V hip joints. Therefore, because of this gap, the numerical method was selected to simulate this hot forging process. Commercial code of Deform 3D was implemented to simulate α phase on all hot forged hip joints. Due to the lack of the sufficient equipment and high cost of fabricating of forging die, the manufacturing and implementation of designed forge die came across with difficulty. Hence, in order to verify the validity of the proposed numerical procedure, simulation of the simple hot compression test on cylindrical specimen on the direction perpendicular to longitudinal axis was performed and the force-displacement curve was compared with the experimental one.

2. Experimental Procedure

The two-phase Ti-6Al-4V titanium alloy used in the present work was produced by casting. Its chemical composition was analyzed using atomic emission spectroscopy (AES).

To perform the hot compression test, the samples were prepared in the form of cylinders with a height of 9 mm, a diameter of 6 mm, and the height to diameter ratio was equal to 1.5 [18]. In order to get a uniform temperature distribution, the lower and upper punches and the sample were placed on the lower punch, and first heated inside the furnace for about 20 min. After performing the hot compression test with the predetermined temperature and strain rate, the samples were quenched in water with a maximum delay of about 5 s so that the microstructural changes in the hot compression test conditions could be observed. Lubrication of the joint surfaces between the punches of the press and the material were performed using a glass strip with a constant friction factor of 0.3 [19]. Hot compression tests were performed at temperatures of 800, 900, 950, and 1000°C, and with strain rates of 0.01, 0.1, and 1 s^{-1} to a total strain of 0.45. To eliminate the effect of friction, in addition to the use of lubricant, the

calculation method based on the upper bound limit criterion and in accordance with procedure explained in reference [20] was used in the stress-strain results.

3. Finite Element Analysis (FEA)

To investigate the hot forging process of hip joint implant and to evaluate the effect of process variables on the volume and distribution of product phases, performing this process numerically before die construction and doing experiments is very valuable. In the present study, numerical simulations using Deform-SFTC software [21] were developed that allow thermomechanical analysis of the forming processes. To this end, the true stress-strain diagram data obtained from hot compression tests were directly implemented to Deform-SFTC software and then the simulations were done. For this purpose, the materials behavior and yield criterion were assumed isotropic, and von-Mises function, respectively.

In order to perform a verification evaluation, similar condition of experimentally done hot compression test was used to simulate it numerically in the Deform-SFTC software and results of force-displacement diagram were compared. For this purpose, the variables of isothermal hot compression test including strain rate and workpiece temperature were determined to be 1 s^{-1} and 900°C, respectively, and finally cooled in water (10 N s^{-1} mm^{-1} $^oC^{-1}$) after the process. Convection coefficient between workpiece and die, convection coefficient to environment, heat capacity, and Poisson's ratio were considered 5 N s^{-1} mm^{-1} $^oC^{-1}$, 0.02 N s^{-1} mm^{-1} $^oC^{-1}$, 565 J/kg°C, and 0.3, respectively. Mesh number, time step for the thermal operations, time step for the thermomechanical operations, punch velocity, and constant friction factor were considered 134000, 0.5 s, 0.05 s, 80 mm/s, and 0.3, respectively. Mesh converging criterion was used to obtain the mesh number. The initial volume fraction of the β and α phases for FEA were considered equal to 10.5 vol.% and 89.5 vol.%, respectively.

There are two main steps in the hot forging of hip joint implants, including: the bending step (preforming) and the forging step (Fig. 1). During the bending step, a cylindrical billet (Fig. 1(a)) is transformed into a preform shape (Fig. 1(b)), and then, through the forging step, the preform is closely transformed into the final shape of the hip joint implant (Fig. 1(c)). The present work focused only on the forging step.

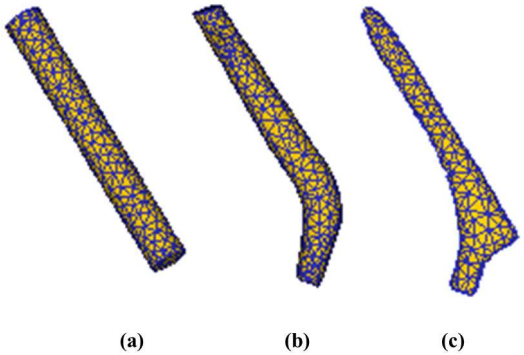

Fig. 1. Steps of forming the hip implant production process; (a) primary billet, (b) bending step (preform), and (c) forging step close to the shape of the final workpiece.

The forging and bending dies were designed through the SolidWorks software [22]. For the purpose of having a real hip joint implant, first its 3D model was designed using the three-dimensional measuring machine and then, after applying dimensional considerations, the final model was obtained. In the design of dies for titanium alloys, due to the high stiffness requirement, the dies were considered rigid in FEA. The most important dimensional considerations in forging die design include machining required thickness, shrinkage, die wear and die wall slope. In this study, 8% of the initial volume and 7 degrees were considered as the excessive thickness and slope angle for the vertical surfaces of the die, respectively. Additionally, a separation line was considered in the middle of the die, so that it divides the cross section of the die into two equal parts. In order to achieve the minimum of the strain non-uniformity and the flash volume, and the maximum amount of die filling, the thickness and width of the flash channel were considered 1.7 mm and 6.5 mm using Noiyberg and Mokel methods [23], respectively. These values are also consistent with the values obtained from the relationship between Brochanov and Rebelsky [23]. Fig. 2 shows the forging die of the hip joint implant considered for simulations and the forged sample inside the die.

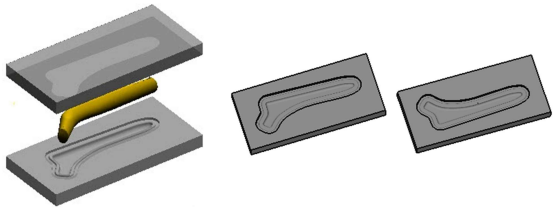

Fig. 2. (a) Hip joint implant forging die and forging preform, (b) lower die, and (c) upper die.

4. Results and Discussion

Table 1 shows the chemical composition of as-received two-phase Ti-6Al-4V titanium alloy. The stress-strain diagrams obtained from the hot-compression test of a two-phase Ti-6Al-4V titanium alloy after elimination of the friction effect are shown in Fig. 3.

Table 1. Chemical composition of two-phase Ti-6Al-4V titanium alloy

Al	V	Cr	Cu	Fe	Mn
5.98	3.94	0.004	0.005	<0.13	<0.004
Mo	**Nb**	**Sn**	**Ni**	**Si**	**Zr**
<0.005	0.008	<0.002	0.007	0.02	0.02
Pb	**Ru**	**C**	**W**	**Ti**	
<0.005	<0.006	<0.005	<0.01	Base	

Fig. 4 shows the force-displacement curves of compression tests done experimentally and by FEA at T = 900ºC and $\dot{\varepsilon}$ =1 s^{-1}. As shown, the process of force changes is almost the same, although due to the simplification of the FEA, deviations between their results were observed, which reaches a maximum of 4.3% in the final stage.

Fig. 5 shows the temperature distribution in the hip joint implant which was forged at 950ºC and a strain rate of 10 s^{-1} on the symmetry level of the workpiece. After the hot forging operation in all simulations, in some parts of the workpiece, higher temperature than the forging temperature was observed. This increase in temperature during the forging process is due to the heat generation in plastic deformation and the heat caused by frictional forces. In parts of the workpiece where the flow of materials is difficult and the flow stress is high, the temperature rises by 10-80ºC.

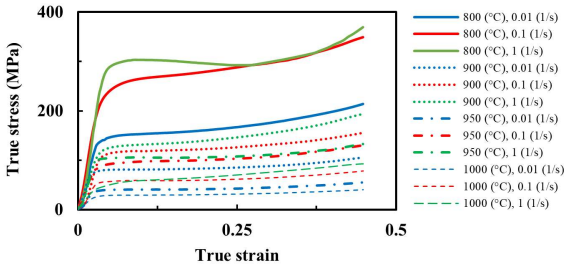

Fig. 3. Effective stress-strain diagram extracted through hot compression test of a two-phase Ti-6Al-4V titanium alloy after friction effect removal.

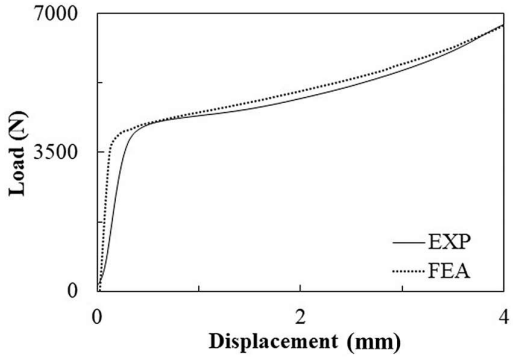

Fig. 4. Force-displacement curves of compression test done experimentally and by FEA at T = 900ºC and $\dot{\varepsilon}$ =1 s^{-1}.

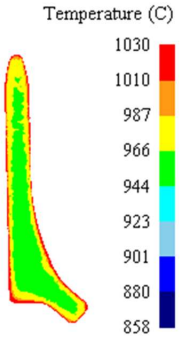

Fig. 5. Temperature distribution in a forged sample of hip joint implant at 950ºC and strain rate of 10 s^{-1} on the symmetry level of the workpiece.

Figs. 6 and 7 show the phase changes and temperature distribution at the end of the forging process, respectively, and Figs. 8 and 9 show the phase changes after the cooling stage at a temperature of 950ºC, a strain rate of 15 s^{-1} and a cooling rate of 30 ºC/s, respectively. During the pre-heating stage, a significant percentage of the α phase was converted to the β phase, and before the bending process, the final β value throughout the workpiece reached about 85 vol.% and the percentage of the α phase reached 15 vol.%. At the end

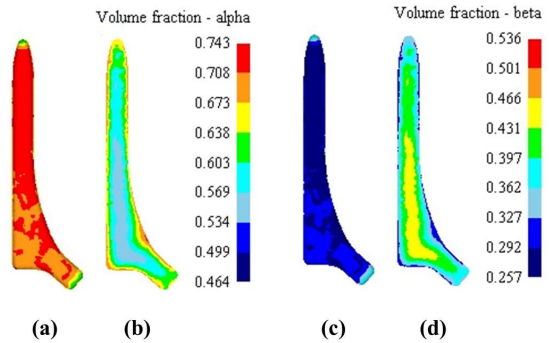

Fig. 6. Phase distribution at the end of the forging process, (a) and (b) final α phase ((a) on the symmetry plane through the center of sample, and (b) on the surface), and (c) and (d) final β phase ((c) on the symmetry plane through the center of sample, and (d) on the surface).

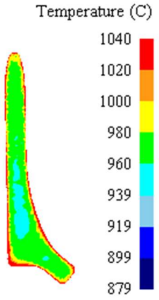

Fig. 7. Temperature distribution in a forged sample of hip joint implant at 950°C and strain rate of 15 s^{-1}.

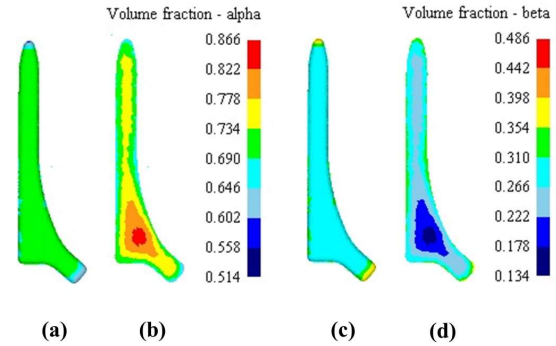

Fig. 8. Phase distributions of forged sample at 950°C, strain rate of 15 s^{-1}, and with the cooling rate of 30 °C/s, (a) vol.% of α, and (b) vol.% of β.

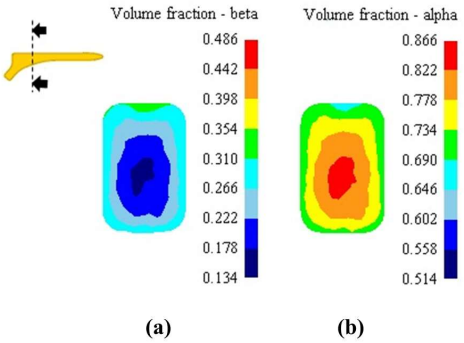

Fig. 9. Phase distributions of forged sample at 950°C, strain rate of 15 s^{-1}, and with the cooling rate of 30 °C/s through cut section, (a) vol.% of β, and (b) vol.% of α.

of the bending process, the lowest percentage of α phase was 38 vol.% and the highest percentage of β phase was 62 vol.% in the center of the workpiece.

Finally, according to Fig. 8, at the end of the forging process the lowest percentage of α phase equal to 46.4 vol.% and the highest percentage of β phase equal to 53.6 vol.% was observed in the center of the workpiece. Due to the temperature difference between the die and the workpiece, the β phase transforms to the α phase during the operation. This increases the α percentage on the surface compared to the center. Moreover, due to the increase in temperature due to deformation and low cooling rate in the center of the workpiece, a lower percentage of the β phase is transformed to the α phase, and finally the β phase is more in the center. It should be noted that before the operation in the heating stage at 950°C, mainly the α phase has been transformed to β throughout the workpiece, and there is less initial α throughout the workpiece.

Regarding Fig. 8, after cooling the workpiece, the remaining β phase transforms into α phase at some points, especially at low cooling rates, resulting in an α + β microstructure. As expected, the amount of the final α phase decreases from the center of the object to the sides due to the contact of the workpiece with the die and the increase of the heat transfer coefficient, and on the contrary, the amount of the final β phase increases from the center of the object to the sides. Therefore, it can be said that there is a lower amount of β phase at the points where α phase is concentrated. These phase changes are clearly shown in the cut section in Fig. 9.

Fig. 10 shows a comparative study of the amount of α phase for temperatures of 850 and 950°C on the symmetry plane (separation plane) and the contact surface with the mold at a strain rate of 10 s^{-1} and a convection coefficient of 20 N s^{-1} mm^{-1} $°C^{-1}$. According to the figure, at the temperature of 850°C, the amount of α phase is higher at the same points in comparison with

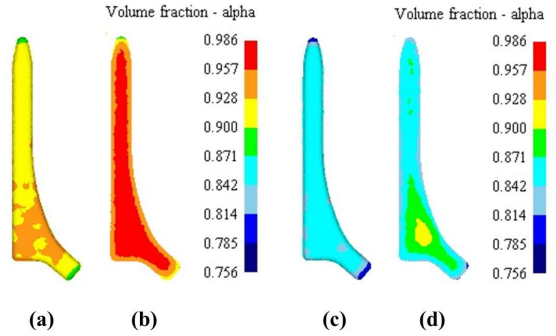

Fig. 10. The volume percentage of α phase at different forging temperatures, (a) and (b) at 850°C ((a) on the symmetry plane through the center of sample, and (b) on the surface), and (c) and (d) at 950°C ((c) on the symmetry plane through the center of sample, and (d) on the surface).

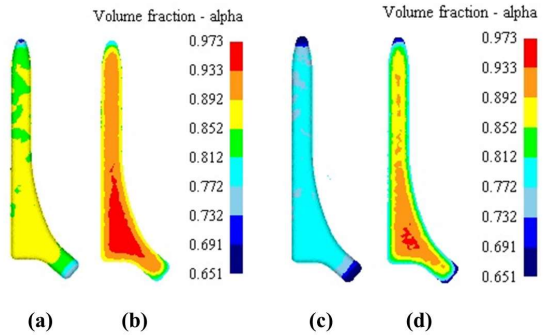

Fig. 11. The volume percentage of α phase at different strain rates, (a) and (b) at 5 s^{-1} ((a) on the symmetry plane through the center of sample, and (b) on the surface), and (c) and (d) at 15 s^{-1} ((c) on the symmetry plane through the center of sample, and (d) on the surface).

the temperature of 950ºC, and in the center of the workpiece, due to the low cooling rate, the highest distribution of α phase is observed.

By examining the effect of the strain rate parameter on the volume fraction of the α phase, it can be seen that with the increase of the strain rate, the percentage of the α phase decreases at all temperatures. The reason for this phenomenon is that when the strain rate increases, large strains occur in contact surfaces with the mold and in parts of the workpiece due to friction and high flow of material. In addition, an increase in the temperature gradient increases the temperature. This increase firstly causes the non-uniform distribution of the α phase throughout the part, and on the other hand, due to the lack of time for cooling during the non-isothermal process, the minimum amount of the final α phase decreases. Fig. 11 shows a comparative study of the amount of α phase for strain rates of 5 and 15 s^{-1} on the symmetry line (separation line) and the contact surface with the mold at a temperature of 900°C and convection coefficient of 20 N s^{-1} mm^{-1} $ºC^{-1}$. As can be seen, at the strain rate of 5 s^{-1}, the minimum and maximum levels of the α phase are higher than they are at the strain rate of 15 s^{-1}. Furthermore, in most of the same places, the percentage of α phase is higher at 850°C.

Additionally, with the increase of the cooling rate, the volume fraction of the α phase decreases. This decrease is because there is not enough time to transform β to stable α phase and martensitic transformation occurs in the α + β Ti-6Al-4V alloy. In other words, β phase is converted to α′ or α″ martensitic phase [24]. While at a lower cooling rate, only diffusional transformation occurs and leads to the formation of a pure α structure. It is worth mentioning that reducing the cooling rate increases the thickness of the α phase layers in the microstructure of the material, which reduces the yield stress and strength of the alloy. In addition, increasing the cooling rate leads to the formation of martensite in the microstructure, and the size of the α layer fibers and the thickness of the α layer decrease. Fig. 12 shows a comparative study of the amount of α phase for a convection coefficient of 10 and 30 N s^{-1} mm^{-1} $ºC^{-1}$ on the symmetry plane (separation plane) and the contact surface with the mold at a temperature of 900°C and a strain rate of 10 s^{-1}. As can be seen, in the convection coefficient of 10 N s^{-1} mm^{-1} $ºC^{-1}$, the amount of α phase in the same points is higher than the convection

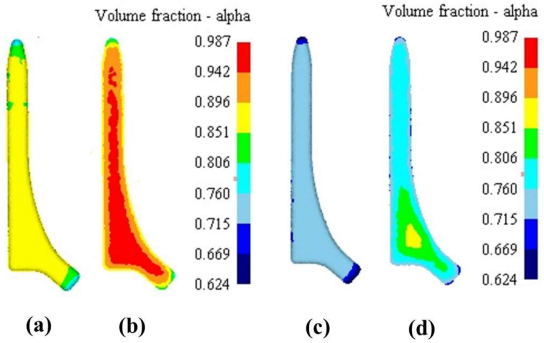

Fig. 12. The volume percentage of α phase at different cooling rates, (a) and (b) at 10 °C/s ((a) on the symmetry plane through the center of sample, and (b) on the surface), and (c) and (d) at 30 °C/s ((c) on the symmetry plane through the center of sample, and (d) on the surface).

coefficient of 30 N s^{-1} mm^{-1} $^{o}C^{-1}$. Moreover, in general, the amount of α phase decreases from the core to the sides. Hence, it can be stated that there is less amount of β phase in the places where there is accumulation of α phase.

5. Conclusion

In this research, first, by using hot compression test, stress-strain curves of the Ti-6Al-4V at temperatures of 800, 900, 950, and 1000°C, and strain rates of 0.01, 0.1, 1 s^{-1} up to strain of 0.45 were obtained. To simulate the distribution of phases in the Ti-6Al-4V forging to a hip joint implant, the data of stress-strain curves were defined and used as the stress-strain behavior of the Ti-6Al-4V alloy in finite element analysis. Then, before the hot forging operation, simulation of the hot compression test of a cylindrical sample made of Ti-6Al-4V was done similar to the conditions of the experiment at a temperature of 900°C and a strain rate of 1 s^{-1}, and the force-displacement curve was compared with the one obtained from the experiment. Verification result showed the accuracy of the finite element analysis used in this research. Finally, to investigate the effect of forging parameters including, temperature, strain rate and cooling rate on the percentage of α and β phases, simulation was done, and the following results were obtained:

- Results showed that all three input variables have an effect on the volume percentage of final α and β phases.
- By increasing the cooling rate, forging temperature and strain rate, the percentage of the final α phase decreases and the amount of the β phase increases.
- Additionally, in all cooling rates, the amount of the final α phase decreases from the center of the object to the sides. It can be said that where there is α phase accumulation, there is less β phase.

Acknowledgements

The authors thank Urmia University, Urmia, Iran for support and access to the research facilities used in this study.

Conflict of Interests

The authors declare no conflict of interest.

Funding

This research received no external funding.

6. References

[1] M. Geetha, A.K. Singh, R. Asokamani, A.K. Gogia, Ti based biomaterials, the ultimate choice for orthopaedic implants–a review, *Progress in Materials Science*, 54(3) (2009) 397-425.

[2] M. Peters, C. Leyens, Titanium and titanium alloys: fundamentals and applications, John Wiley & Sons, 2006.

[3] R.K. Nalla, R.O. Ritchie, B.L. Boyce, J.P. Campbell, J.O. Peters, Influence of microstructure on high-cycle fatigue of Ti-6Al-4V: bimodal vs. lamellar structures, *Metallurgical and Materials Transactions A*, 33(3) (2002) 899-918.

[4] J.H. Zuo, Z.G. Wang, E.H. Han, Effect of microstructure on ultra-high cycle fatigue behavior of Ti–6Al–4V, *Materials Science and Engineering: A*, 473(1-2) (2008) 147-152.

[5] G.Q. Wu, C.L. Shi, W. Sha, A.X. Sha, H.R. Jiang, Effect of microstructure on the fatigue properties of Ti-6Al-4V titanium alloys, *Materials & Design*, 46 (2013) 668-674.

[6] V. Crupi, G. Epasto, E. Guglielmino, A. Squillace, Influence of microstructure [alpha+ beta and beta] on very high cycle fatigue behavior of Ti-6Al-4V alloy, *International Journal of Fatigue*, 95 (2017) 64-75.

[7] M. Niinomi, M. Nakai, J. Hieda, Development of new metallic alloys for biomedical applications, *Acta Biomaterialia*, 8(11) (2012) 3888-3903.

[8] S.H. Teoh. Fatigue of Biomaterials: a review, *International Journal of Fatigue*, 22(10) (2000) 825-837.

[9] L.R. Saitova, H.W. Höppel, M. Göken, I.P. Semenova, G.I. Raab, R.Z. Valiev, Fatigue behavior of ultrafine-grained Ti–6Al–4V 'ELI' alloy for medical applications, *Materials Science and Engineering: A*, 503(1-2) (2009) 145-147.

[10] J.B. Park, R.S. Lakes, Metallic implant materials, *Biomaterials*, (2007) 99-137.

[11] M. Semilitsch, H.G. Willert, Properties of implant alloys for artificial hip joints, *Medical and Biological Engineering and Computing*, 18(4) (1980) 511-520.

[12] D.R. Sumner, T.M. Turner, R. Igloria, R.M. Urban, J.O. Galante, Functional adaptation and ingrowth of bone vary as a function of hip implant stiffness, *Journal of Biomechanics*, 31(10) (1998) 909-917.

[13] M. Long, H.J. Rack, Titanium alloys in total joint replacement—a materials science perspective, *Biomaterials*, 19(18) (1998) 1621-1639.

[14] M. Balazic, J. Kopac, M.J. Jackson, W. Ahmed, Titanium and titanium alloy applications in medicine, *International Journal of Nano and Biomaterials*, 1(1) (2007) 3-34.

[15] A.K. Mishra, J.A. Davidson, R.A. Poggie, P. Kovacs, T.J. FitzGerald, Mechanical and tribological properties and biocompatibility of diffusion hardened Ti-13Nb-13Zr—a new titanium alloy for surgical implants, *Medical Applications of Titanium and Its Alloys: The Material and Biological Issues, ASTM International*, (1996) 96-113.

[16] M. Semlitsch, Titanium alloys for hip joint replacements, *Clinical Materials*, 2(1) (1987) 1-13.

[17] H. Gheshlaghi, V. Alimirzaloo, M. Shahbaz, A. Amiri, Numerical study and optimization of the thermomechanical procedure in forging of two-phase Ti-6Al-4V Alloy for artificial hip joint implant, *Iranian Journal of Materials Forming*, 9(3) (2022) 31-43.

[18] ASM Metals Handbook Vol. 14: Forming and Forging, ASM International, 9th Edition, 1988.

[19] R. Sethy, L. Galdos, J. Mendiguren, E. Sáenz de Argandoña, Friction and heat transfer coefficient determination of titanium alloys during hot forging conditions, *Advanced Engineering Materials*, 19(6) (2017) 1600060.

[20] R. Ebrahimi, A. Najafizadeh, A new method for evaluation of friction in bulk metal forming, *Journal of Materials Processing Technology*, 152(2) (2004) 136-143.

[21] Scientific Forming Technologies Corporation (SFTC), 2010.

[22] S.K. Choi, M.S. Chun, C.J. Van Tyne, Y.H. Moon, Optimization of open die forging of round shapes using FEM analysis, *Journal of Materials Processing Technology*, 172(1) (2006) 88-95.

[23] V. Alimirzaloo, F.R. Biglari, M.H. Sadeghi, Numerical and experimental investigation of preform design for hot forging of an aerofoil blade, *Proceedings of the Institution of Mechanical Engineers, Part B: Journal of Engineering Manufacture*, 225(7) (2011) 1129-1139.

[24] J. Sieniawski, W. Ziaja, K. Kubiak, M. Motyka, Microstructure and mechanical properties of high strength two-phase titanium alloys, Titanium Alloys-Advances in Properties Control, InTech, Croatia, 2013, pp. 69-80.